

Supplementary Materials for

Variable gene expression and parasite load predict treatment outcome in cutaneous leishmaniasis

Camila Farias Amorim, Fernanda O. Novais, Ba T. Nguyen, Ana M. Misic, Lucas P. Carvalho, Edgar M. Carvalho, Daniel P. Beiting*, Phillip Scott*

*Corresponding author. Email: beiting@upenn.edu (D.P.B.); pscott@upenn.edu (P.S.)

Published 20 November 2019, *Sci. Transl. Med.* **11**, eaax4204 (2019)
DOI: 10.1126/scitranslmed.aax4204

The PDF file includes:

- Fig. S1. Top 100 up-regulated genes in CL lesions relative to healthy skin.
- Fig. S2. Age, sex, lesion size, and delayed-type hypersensitivity response are not associated with treatment failure.
- Fig. S3. CombiROC analysis identifies gene combinations for accurately predicting treatment outcome.
- Fig. S4. Absolute quantification of *L. braziliensis* parasites in CL lesions by qPCR.
- Fig. S5. Relative abundance of parasite transcripts correlates with expression of eight ViTALs.
- Fig. S6. Non-ViTAL genes do not correlate with parasite load.
- Fig. S7. Coverage plot for *L. braziliensis* read mapping.
- Fig. S8. Model showing proposed role of parasite load in determining treatment outcome in CL.
- Table S1. Demographic and clinical metadata from patients with CL.

Other Supplementary Material for this manuscript includes the following:

(available at stm.sciencemag.org/cgi/content/full/11/519/eaax4204/DC1)

- Data file S1 (Microsoft Excel format). GO enrichment analysis results for 250 ViTALs.
- Data file S2 (.pdf file). Supplementary code file.

Supplementary Materials

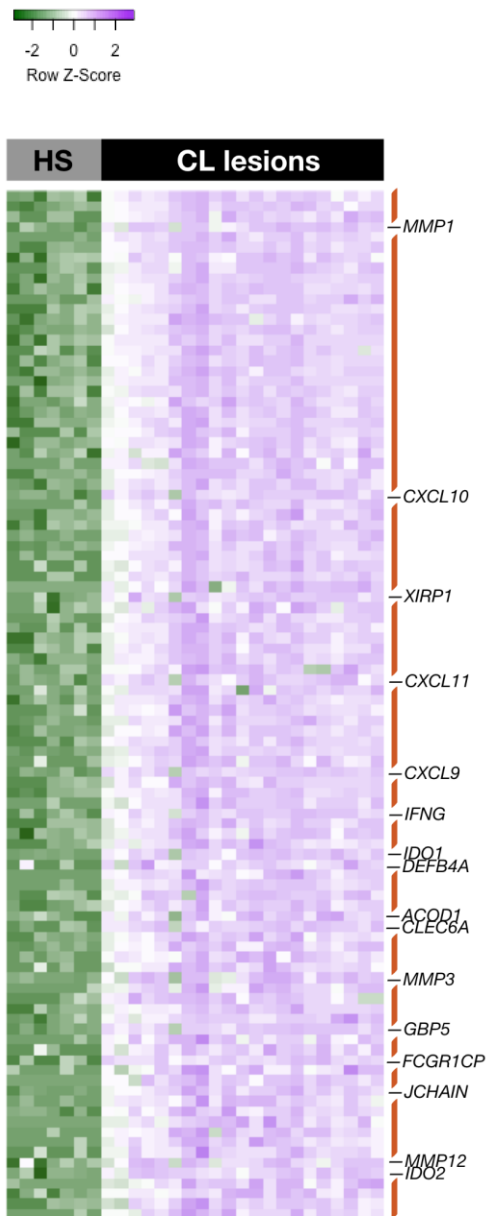


Fig. S1. Top 100 up-regulated genes in CL lesions relative to healthy skin. Heatmap with columns and rows representing individual samples and genes, respectively. Heatmap color reflects row z-scores of gene expression across samples. Genes are listed in descending order by fold change (FC). Red side bars indicate location of immunoglobulin-related genes. DEGs, differentially expressed genes; CL lesions, cutaneous leishmaniasis lesions; HS, healthy skin; CPM, counts per million; FC, fold change.

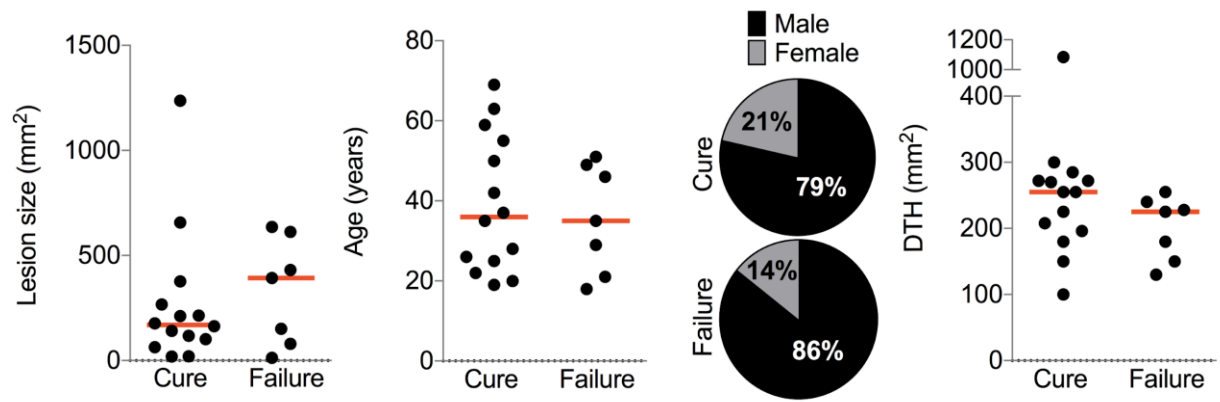


Fig. S2. Age, sex, lesion size, and delayed-type hypersensitivity response are not associated with treatment failure. Demographic and clinical metadata recorded on Day 0 from CL patients who were cured (n=14) or for whom treatment failed (n=7) after the first round of treatment. DTH, delayed-type hypersensitivity test.

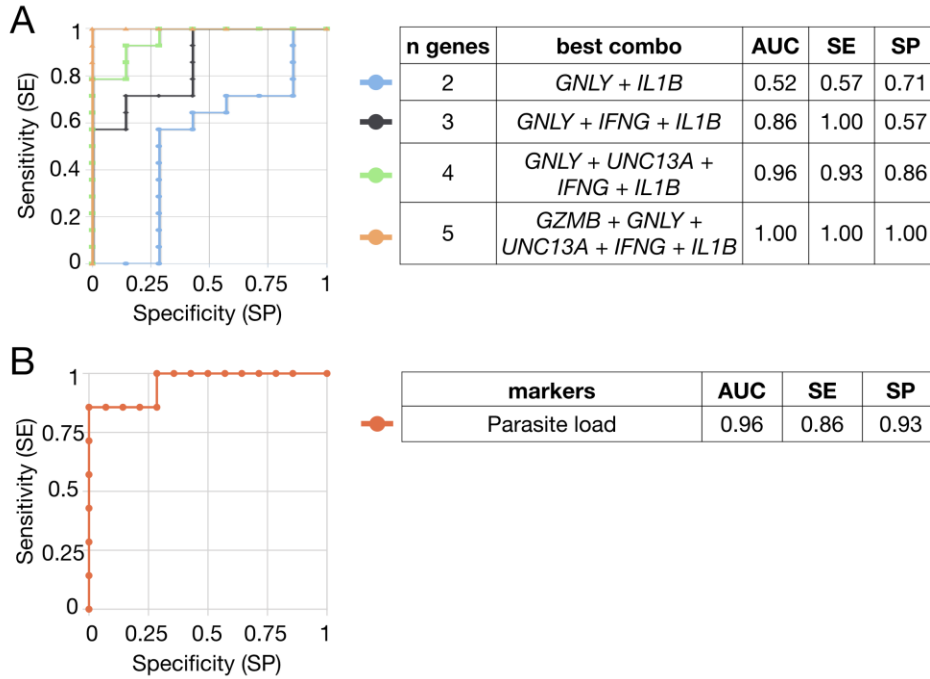


Fig. S3. CombiROC analysis identifies gene combinations for accurately predicting treatment outcome.

(A) CombiROC software was used to generate ROC for the best combination of genes (*GZMB*, *PRF1*, *GNLY*, *IL1B*, *APOBEC3A*, *UNC13A*, *KIR2DL4*, *CCL4*) for predicting treatment outcome in the current cohort of patients. (B) ROC analysis using parasite load only. Axes represent the sensitivity (true negative rate, SE) and specificity (false positive rate, SP). ROC, receiver operating curve; AUC, area under the curve; SE, sensitivity; SP, specificity.

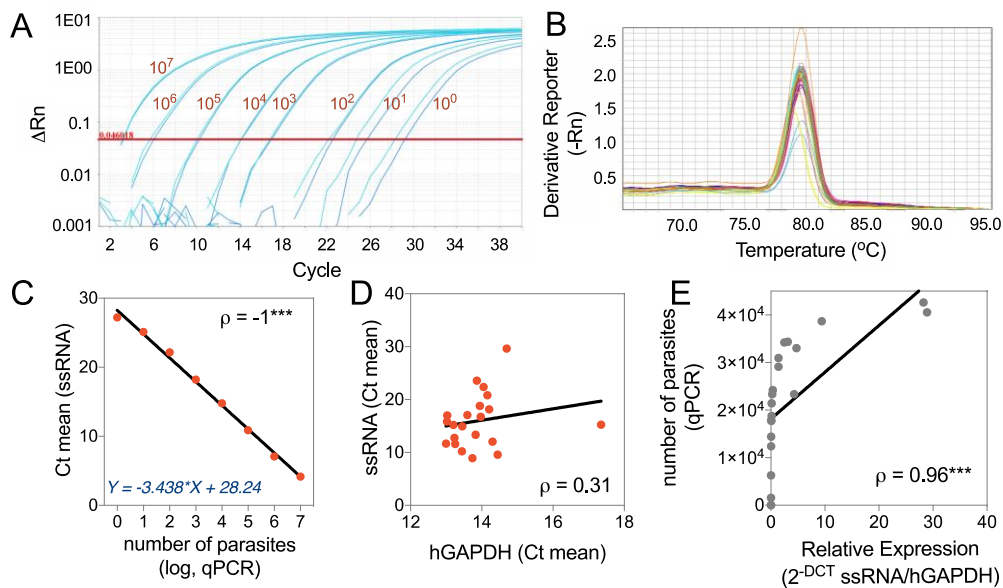


Fig. S4. Absolute quantification of *L. braziliensis* parasites in CL lesions by qPCR. RNA extracted from 4mm lesion biopsies was converted to cDNA and used to quantify parasite 18S ribosomal subunit (ssRNA). Human *GAPDH* was used as an internal housekeeping gene control. **(A)** Standard curve produced using RNA extracted from cultured promastigotes. ΔRn value of the parasite standard curve assayed in duplicate. **(B)** Melt curve from ssRNA amplification of standard curve and CL biopsies (n=21). **(C)** Linear regression and Spearman's correlation for parasite standard curve. The equation used to interpolate the absolute number of parasites in skin biopsies from a standard curve is shown in blue. **(D)** Correlation between Ct mean values of ssRNA and hGAPDH. **(E)** Correlation between absolute number of parasites in the biopsy and relative expression of ssRNA normalized to hGAPDH Ct mean value. Spearman's test was used for correlation analysis. ρ , Spearman's rho correlation coefficient; * $P < 0.05$, ** $P < 0.01$, *** $P < 0.001$; qPCR assay, quantitative polymerase chain reaction assay; ΔRn , delta normalized reporter value.

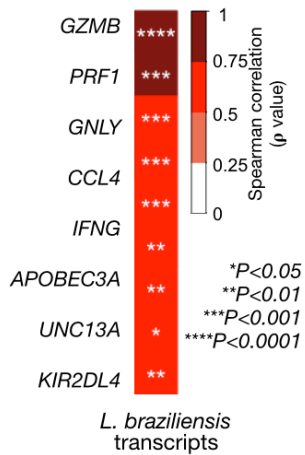


Fig. S5. Relative abundance of parasite transcripts correlates with expression of eight ViTALs.

Correlation matrix comparing expression of potential biomarkers (left) with the relative abundance of *L. braziliensis* transcripts measured in the same sample by dual-RNAseq. Spearman's test was used for correlation analysis. ρ , Spearman's rho correlation coefficient; * $P < 0.05$, ** $P < 0.01$, *** $P < 0.001$ and **** $P < 0.0001$.

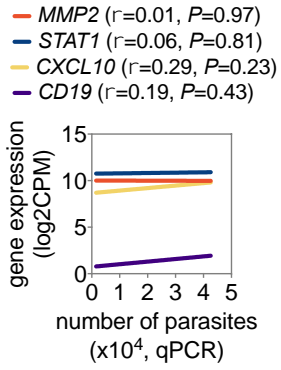


Fig. S6. Non-ViTAL genes do not correlate with parasite load. Correlation analysis comparing parasite load measured by qPCR, with the expression of representative non-ViTAL genes selected based on their established role in the immune response during cutaneous leishmaniasis. Spearman's test was used for correlation analysis. ρ , Spearman's rho correlation coefficient.

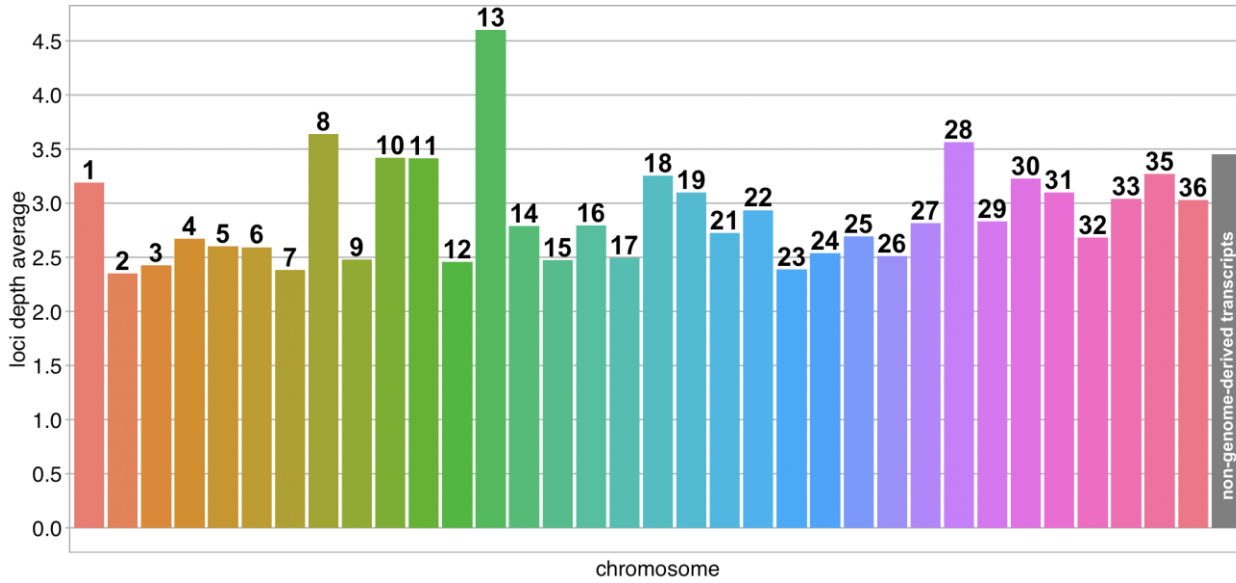


Fig. S7. Coverage plot for *L. braziliensis* read mapping. After filtering to remove host reads, remaining reads were mapped to the *Leishmania braziliensis* cDNA reference transcriptome (MHOM/BR/75/M2904). Representative coverage plot showing average read coverage for each chromosome from sample CL1.

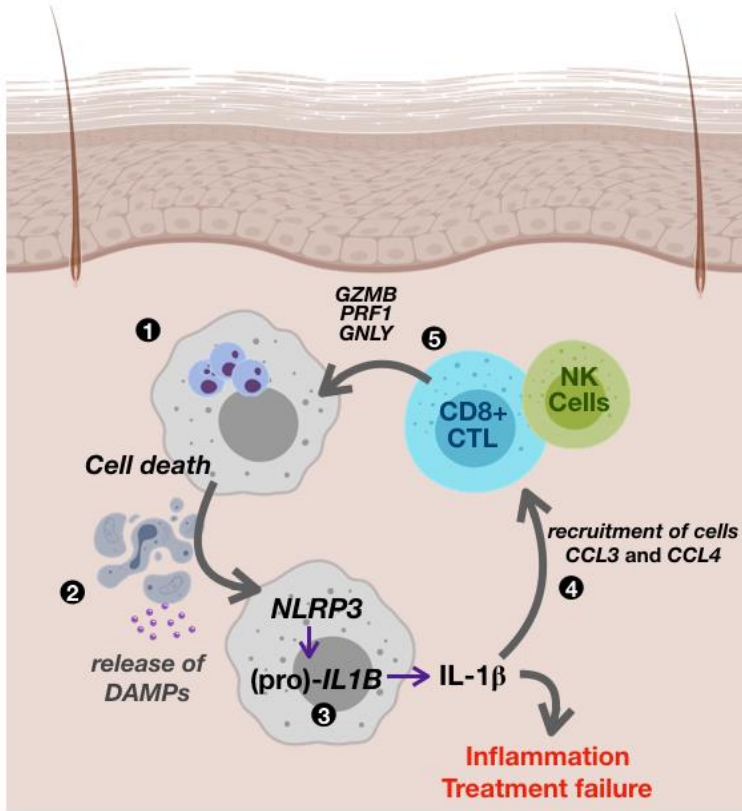


Fig. S8. Model showing proposed role of parasite load in determining treatment outcome in CL. 1) In lesions from patients with a increased number of intracellular parasites, infected cells are targets for CD8+ effector T cells expressing *GZMB*, *PRF1* and *GNLY*. 2) Damage-associated molecular patterns (DAMPs) are released from the target cells following lysis by CD8+ T cells, which 3) activate the inflammasome complex in cells within the lesion. This activation induces the expression, maturation and release of IL-1 β which is responsible for increased inflammation and skin damage, leading to greater overall time to heal the lesion (treatment failure). 4) IL-1 β also has the ability of stimulate a diverse set of effector cells in the lesion to produce chemokines (CCL3 and CCL4) and 5) recruit more cytotoxic effector cells (CD8+ effector T cells and NK cells) to the site of infection, thus further exacerbating the inflammation.

Table S1. Demographic and clinical metadata from patients with CL. Sample identifier, treatment outcome information, age (years), sex, DTH (mm²), lesion size (mm²) and time to cure (days) for each lesion sample.

CL, cutaneous leishmaniasis; DTH, delayed-type hypersensitivity test.

sample	disease	treatment_outcome	age_(years)	sex	DTH_(mm2)	lesion_size_(mm2)	Time_to_cure_(days)
host_HS01	control	na	na	na	na	na	na
host_HS02	control	na	na	na	na	na	na
host_HS03	control	na	na	na	na	na	na
host_HS04	control	na	na	na	na	na	na
host_HS05	control	na	na	na	na	na	na
host_HS06	control	na	na	na	na	na	na
host_HS07	control	na	na	na	na	na	na
host_CL01	cutaneous	failure	35	F	255	79	150
host_CL02	cutaneous	failure	21	M	228	613	130
host_CL03	cutaneous	failure	29	M	180	393	150
host_CL04	cutaneous	cure	37	M	300	19	40
host_CL05	cutaneous	cure	50	M	272	212	80
host_CL06	cutaneous	cure	26	F	285	102	90
host_CL07	cutaneous	cure	28	F	272	163	45
host_CL08	cutaneous	cure	63	M	196	214	62
host_CL09	cutaneous	cure	59	M	255	267	70
host_CL10	cutaneous	cure	22	M	255	657	75
host_CL11	cutaneous	failure	49	M	240	13	140
host_CL12	cutaneous	cure	42	M	225	141	54
host_CL13	cutaneous	cure	69	M	150	177	60
host_CL14	cutaneous	cure	19	M	208	377	45

host_CL15	cutaneous	failure	18	M	130	151	150
host_CL16	cutaneous	failure	46	M	150	431	135
host_CL17	cutaneous	cure	35	M	270	20	90
host_CL18	cutaneous	failure	51	M	225	636	203
host_CL19	cutaneous	cure	25	M	180	118	60
host_CL20	cutaneous	cure	20	F	100	63	80
host_CL21	cutaneous	cure	55	M	1085	1237	70